New Phytologist

Research

Nectary photosynthesis contributes to the production of mānuka (*Leptospermum scoparium*) floral nectar

Michael J. Clearwater[1], Stevie T. Noe[1], Merilyn Manley-Harris[1], Georgia-Leigh Truman[1], Stephen Gardyne[1], Jessica Murray[1], Sylvester A. Obeng-Darko[1,2] and Sarah J. Richardson[3]

[1]Te Aka Mātuatua – School of Science, University of Waikato, Hamilton 3216, New Zealand; [2]School of Biological Science, University of Western Australia, Perth, WA 6009, Australia; [3]Manaaki Whenua – Landcare Research, PO Box 69040, Lincoln 7640, New Zealand

Author for correspondence:
Michael J. Clearwater
Email: m.clearwater@waikato.ac.nz

Received: *6 April 2021*
Accepted: *4 July 2021*

New Phytologist (2021) **232:** 1703–1717
doi: 10.1111/nph.17632

Key words: dihydroxyacetone, flower, light, Mānuka (*Leptospermum scoparium*), nectar, nectary, photosynthesis.

Summary

- Current models of floral nectar production do not include a contribution from photosynthesis by green nectary tissue, even though many species have green nectaries. Mānuka (*Leptospermum scoparium*) floral nectaries are green, and in addition to sugars, their nectar contains dihydroxyacetone (DHA), the precursor of the antimicrobial agent in the honey. We investigated causes of variation in mānuka floral nectar production, particularly the effect of light incident on the nectary.
- Flower gas exchange, chlorophyll fluorescence, and the effects on nectar of age, temperature, light, sucrose, 3-(3,4-dichlorophenyl)-1,1-dimethylurea (DCMU), pyridoxal phosphate, and $^{13}CO_2$, were measured for attached and excised flowers.
- Flower age affected all nectar traits, whilst temperature affected total nectar sugar only. Increased light reduced floral CO_2 efflux, increased nectar sugar production, and affected the ratio of DHA to other nectar sugars. DCMU, an inhibitor of photosystem II, reduced nectar sugar production. Pyridoxal phosphate, an inhibitor of the chloroplast envelope triose phosphate transporter, reduced nectar DHA content. Incubation of excised flowers with $^{13}CO_2$ in the light resulted in enrichment of nectar sugars, including DHA.
- Photosynthesis within green nectaries contributes to nectar sugars and influences nectar composition. Mānuka nectar DHA arises from pools of triose phosphate that are modulated by nectary photosynthesis.

Introduction

Floral nectar is a complex secretion produced by a specialized tissue, the nectary, and awarded to animals in return for their pollination services (Pacini & Nicolson, 2007). Nectar usually contains sucrose, glucose, and fructose in varying proportions, along with smaller amounts of a wide variety of other compounds, including other sugars, amino acids, proteins, lipids and secondary metabolites (Percival, 1961; Nicolson & Thornburg, 2007; Roy *et al.*, 2017). Nectar volume, concentration and composition vary widely among species, with important implications for plant–pollinator interactions (Chalcoff *et al.*, 2006; Wolff, 2006; Witt *et al.*, 2013; Nepi, 2017; Parachnowitsch *et al.*, 2019). Within species, nectar is usually consistent in terms of the proportions of the dominant sugars, but can also vary significantly in composition among flowers and individual plants (Nicolson & Thornburg, 2007; Noe *et al.*, 2019). Much of this variation in nectar chemistry may be linked to the mechanism responsible for nectar secretion – how it differs between species, how it changes during flower development, and how it is modulated by the environment (Roy *et al.*, 2017).

Floral nectaries have evolved multiple times, and exhibit a variety of mechanisms for nectar secretion (Bernardello, 2007; Heil, 2011; Roy *et al.*, 2017). The best understood models for nectar secretion are based on fast growing species with short-lived flowers and rapid nectar secretion, including *Arabidopsis* (Kram & Carter, 2009) and *Nicotiana* (Ren *et al.*, 2007; Thornburg, 2007). These species exhibit an eccrine-based secretion of the major nectar sugars, whereby sugar is exported across the plasma membrane of the nectary parenchyma via membrane pores or transporters (Lin *et al.*, 2014), and their nectaries are either non-green (*Nicotiana*), or pale green (*Arabidopsis*), and shaded within the flower. Phloem supplied sugar accumulates as starch in amyloplasts or amylochromoplasts, and a brief surge of nectar secretion (hours to 1 or 2 d) at anthesis is supplied by starch degradation (Horner *et al.*, 2007; Ren *et al.*, 2007; Lin *et al.*, 2014). Nectar production from starch may also be supplemented by simultaneous direct import of sugars from the phloem (Solhaug *et al.*, 2019). However, the nectaries of many other species are green, contain chloroplasts rather than amyloplasts, and accumulate little or no starch before or after anthesis (Davis *et al.*, 1986; Davis *et al.*, 1988; O'Brien *et al.*, 1996; Vesprini *et al.*, 1999; Vezza *et al.*, 2006; Nepi, 2007). Pacini *et al.* (2003)

associated these types of nectaries with longer lived flowers that produce nectar more slowly and over extended periods (a few to many days), and proposed that photosynthesis within the nectary itself could supply some or all of the sugars required for nectar production. Based on chlorophyll fluorescence, green nectaries are theoretically capable of fixing a significant proportion of total nectar sugars (Lüttge, 2013), but there is no direct evidence that *de novo* photosynthesis within green nectaries contributes to nectar production (Roy *et al.*, 2017). Nectary photosynthesis by green nectaries could explain aspects of variation in nectar composition and the origin of particular nectar compounds.

Mānuka (*Leptospermum scoparium*) is a perennial woody shrub that produces long lived flowers with green nectaries (Fig. 1; Clearwater *et al.*, 2018). Mānuka flowers are dish shaped with the nectaries exposed to light on the upper surface of the gynoecium when the flower opens (Fig. 1). In addition to fructose, glucose and sucrose, the floral nectar of mānuka and a subset of other *Leptospermum* species contains small amounts of dihydroxyacetone (DHA) (Williams *et al.*, 2018), a three carbon sugar that is the precursor of the nonperoxide antibacterial activity of mānuka honey (Adams *et al.*, 2008; Mavric *et al.*, 2008; Adams *et al.*, 2009). The DHA content of mānuka nectar is highly variable, with some of this variation attributed to plant genotype, flower stage of development, temperature, and differential resorption of nectar components (Williams *et al.*, 2014; Clearwater *et al.*, 2018; Smallfield *et al.*, 2018; Noe *et al.*, 2019). The source and function of DHA in mānuka nectar remains unknown (Clearwater *et al.*, 2018). Little or no starch is observed within the mānuka nectary before or after anthesis, and nectar is produced for around 14 d after anthesis (Clearwater *et al.*, 2018; Obeng-Darko, 2018). Clearwater *et al.* (2018) proposed that the source of DHA within mānuka nectary secretory cells was cytoplasmic pools of DHA phosphate (and its triose-phosphate isomer, glyceraldehyde 3-phosphate). Triose-phosphate is an important intermediate in primary metabolism, and in green plant cells triose phosphate is the product of the Calvin cycle that is exported to the cytoplasm by chloroplasts while they are exposed to light (Flugge, 1999). This hypothesis suggests that exposure of the nectary to light should affect both total nectar sugar production, and nectar DHA content. An alternative hypothesis for the origin of DHA in mānuka nectar is that it is a metabolite produced by endophytic or nectar inhabiting microbes (Williams *et al.*, 2014). A number of bacteria and fungi are capable of producing DHA from a range of precursors (Macauley *et al.*, 2001; Russmayer *et al.*, 2015), and mānuka is known to host an extensive microbiome that influences plant growth and chemistry (Wicaksono *et al.*, 2016; Wicaksono *et al.*, 2017; Thrimawithana *et al.*, 2019).

The hypothesis tested in this study was that nectary photosynthesis contributes to nectar production by mānuka, and that nectar amount and composition, including DHA content, are influenced by treatments that affect photosynthesis. Previous research demonstrated that stage of flower development influences nectar flow and composition (Clearwater *et al.*, 2018; Smallfield *et al.*, 2018). We therefore conducted a more detailed investigation of the effect of nectar sampling time, temperature and light, on nectar production by attached flowers. Resampling flowers with differing frequencies tested the effects of nectar resorption. The effect of light incident on the nectary was further investigated using excised flowers, after it was found that mānuka flowers produce nectar for at least 24 h after excision if incubated under appropriate conditions. Flower CO_2 exchange, varied lighting, sucrose supply and inhibitors of chloroplast activity were used to test the role of photosynthesis in nectar and DHA production, and $^{13}CO_2$ was used as a tracer to determine whether carbon assimilated by the flower itself was incorporated into nectar sugars. Based on the results, a modified biochemical model of nectary sugar production is proposed for species with green

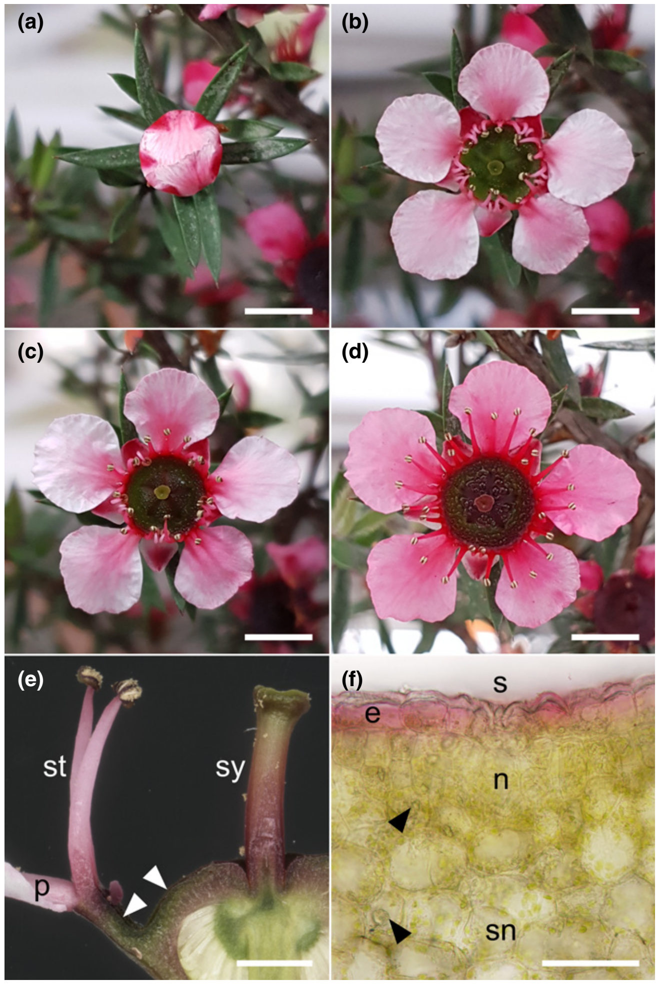

Fig. 1 Mānuka (*Leptospermum scoparium*) floral nectary morphology and anatomy. (a–e) Example of an *L. scoparium* cv. 'Martinii' (*L.* 'Martinii') flower imaged 1 d before anthesis (a), and the same flower on the day of anthesis (b), 1 d after anthesis (c) and 4 d after anthesis (d) showing accumulation of nectar and the darkening of the nectary surface from green to red. (e) Half-flower slice of an *L.* 'Martinii' flower on the day after anthesis, showing the green nectary tissue on the wall of the gynoecium and staminophore (arrowheads). p, petal; st, stamen; sy, style. (f) Unstained transverse hand-section of the staminophore on the day after anthesis, with abundant green chloroplasts in the nectary parenchyma, a nectary stoma, and accumulation of red pigmentation in the epidermis. Druse crystals are also present (arrowheads). s, stomata; n, nectary parenchyma; sn, sub-nectary parenchyma; e, epidermis. Bars, 5 mm (a–d), 1.5 mm (e), 50 μm (f).

nectaries that incorporates the contribution of nectary chloroplasts to nectar sugars.

Materials and Methods

Plant materials and glasshouse conditions

Hermaphrodite flowers of the clonally propagated horticultural cultivar *Leptospermum scoparium* cv. 'Martinii' (*L.* 'Martinii') were used for all experiments. *L.* 'Martinii' is triploid and is thought to be the result of a cross between *L. scoparium* 'Keatleyii' and *L. scoparium* 'Nichollsii' (Dawson, 2010). *Leptospermum scoparium* cv. 'Martinii' was selected because it is highly floral, has a long flowering period, and produces relatively large and open flowers that facilitate nectar sampling (Clearwater *et al.*, 2018). As observed in most other genotypes of *L. scoparium*, the upper surface of the gynoecium and staminophore of *L.* 'Martinii' flowers, including the nectary tissue (referred to collectively as the hypanthium), is green when the flower opens, but begins to darken as red pigments accumulate in vacuoles of the epidermis and underlying tissues within 1 to 2 d of opening (Fig. 1a–d). Chloroplasts are abundant in the green nectary parenchyma located beneath the nectary stomata (Fig. 1e,f). Plants for all experiments were kept in pots outdoors, before being moved into the glasshouse and acclimatized for 1 wk prior to starting experiments. Plants were 1 to 3 yr old and grown in 2 to 9 l pots.

The glasshouse was equipped with an automated control system connected to heating, ventilation, evaporative cooling and irrigation. Daylength was extended to 15 h using sodium vapour grow lights during the flower age experiment, and 10 to 11 h during the flower shading and temperature experiments. Glasshouse environmental control was set to maintain daytime temperature between 18 and 24°C, humidity above 50%, and nocturnal temperature above 8–10°C, except during the temperature experiment.

Nectar sampling

For all experiments, nectar was collected from flowers using a rinsing (pipetting) method similar to that of Mallick (2000). An auto-pipette was used to gently pipette 10 µl of distilled water onto the open nectary surface, then re-collect the liquid into a pre-weighed sample tube, without causing damage to the nectary surface. The 10 µl rinse was repeated once so that 20 µl in total was used to remove nectar from each flower. Sample tubes were re-weighed, and the sample mass and volume determined by subtracting the pre-weighed empty tube mass from the tube plus sample mass and assuming a density of 1 g ml^{-1}, based on the observation that sugar content was 3% or less. Sample tubes were stored at −20°C until further analysis.

Flower age and frequency of nectar sampling

Nectar yield and composition were measured as a function of flower age and the frequency of nectar removal. Flower buds were tagged and opening date recorded on 20 plants. An open flower was defined as having the tips of two or more petals unfurled from the underlying petals. Flowers were grouped into cohorts of the same age, then into sample units of 10 to 12 flowers from which nectar was pooled into a single sample. Sample units were assigned to either 2, 4 or 6 d nectar sampling frequencies, and the same flowers were sampled repeatedly in the afternoon using the rinsing method until nectar production ceased after approximately 16 d. There were four to six sample units per sampling frequency, and units were spread across plants.

Temperature effect on nectar flow

Fourteen plants in 9 l pots (2–3 yr old, 60 cm in height) were selected, and one nectar sampling unit of 10 newly opened flowers of the same age was labelled per plant. At 4 d after flower opening, with all 14 plants in a single room without heating, nectar was removed at 4 p.m. from all flowers and discarded. The plants were then distributed between three glasshouse rooms and subjected to 24-h temperature profiles 2, 4 and 6°C above outside ambient temperature. After each 24 h period, nectar was resampled from the same flowers and plants randomly assigned to another room with a different temperature regime, for four consecutive days. Humidity and lighting were allowed to vary naturally. The actual temperatures achieved in each room was used as the independent variable for comparison with nectar production.

Shading flowers on-plant

Individual intact flowers were shaded *in situ* on plants in the glasshouse. On three plants, 21 flower buds were labelled per plant, the opening date of each flower was recorded, and seven flowers were randomly assigned to each of three treatment groups: uncovered, covered with plastic film (transparent plastic film, admitted light but decreased evaporation), or covered with aluminium foil (excluded light and decreased evaporation). Covered treatments were applied immediately after flower opening and only the flower was covered, without covering of nearby shoots or leaves. Flowers were left covered until a single nectar sample was taken from each sample unit by rinsing the seven flowers per treatment on each plant, between 5 and 9 d after flower opening.

Flower photosynthesis

Carbon dioxide exchange by excised flowers, cut from the plant 2–6 d after anthesis, was measured with a differential photosynthesis system (LI6400XT; Li-Cor, Lincoln, NE, USA) equipped with a bryophyte chamber (LI6400-24) and light emitting diode (LED) light source (LI6400-18A). Eight to ten flowers were enclosed within the chamber at the same time, with their upper gynoecial surfaces and nectaries facing upwards (towards the light), and their cut pedicels submerged in water. Flower temperature was maintained at 20 ± 1.5°C and relative humidity between 50 and 70%. Preliminary measurements indicated that gas exchange rates remained constant for at least 6 h after excision. Light and CO_2 response curves were recorded by varying the photosynthetic photon flux density (PPFD) between 2000 and 0 μmol m^{-2} s^{-1}, with reference CO_2 held constant at 400 ppm, and then later the reference CO_2 varied between 50 and 1200 ppm, with PPFD held constant at 500 μmol m^{-2} s^{-1}. Response curves were repeated with new flowers seven times, including twice with only flowers that had green hypanthiums, and five times with only flowers that had darker (generally older) hypanthiums. On three occasions, after completing measurements on whole flowers, the nongreen stamens, petals and sepals were removed and measurements repeated with only the gynoecium and hypanthium inside the chamber.

A pulse amplitude modulated fluorometer (Mini-PAM; Walz, Germany) was used to measure chlorophyll fluorescence of the leaves and nectaries of attached flowers with red hypanthiums, as described by Lüttge (2013). The automated light response procedure of the instrument was used to estimate the effective quantum yield of photosystem II, and the apparent electron transport rate of photosystem II, while PPFD was varied. Chlorophyll fluorescence measurements were also used to monitor the photosynthetic activity of the nectaries of excised flowers while they were incubated with and without 100 μM 3-(3,4-dichlorophenyl)-1,1-dimethylurea (DCMU; an inhibitor of photosystem II) added to their water supply (see Excised flower experiments).

Excised flower experiments

For excised flower experiments, flowers were detached from multiple plants, provided with distilled water or water containing sucrose (30 g l^{-1}) (vase solution; Burge *et al.*, 1996), and exposed to controlled levels of irradiance while they produced nectar at a constant temperature of 20°C. Newly opened flowers were labelled on the plant and harvested 3–4 d after opening, with nectar removed and discarded using the rinsing method immediately prior to excision. Flowers were excised at the base of the receptacle and each placed in a hole in a plastic tray floating in the incubation solution within a plastic container, so that the receptacle was immersed in solution. The incubation chambers were covered with a clear acrylic sheet to maintain a high humidity, and white light supplied from above using dimmable LED strip lighting. Irradiance was measured as PPFD at the level of the flower using a quantum sensor. During the experiments, incubation chambers were kept in temperature-controlled boxes with gynoecium temperature, measured using a thermocouple, maintained at 20°C. Dark treatments were achieved by wrapping individual incubation chambers in aluminium foil. To determine whether sucrose added to the incubation solution could be incorporated into nectar, nectar sugars were harvested from flowers incubated in the light and supplied with either water or the sucrose solution prepared from cane sugar (30 g l^{-1} of C4 sucrose, naturally enriched in carbon-13 (^{13}C) compared to sugars from C3 species such as *L. scoparium*). Three nectar samples, each containing nectar pooled from 10 flowers, were collected per treatment. The cane sugar and harvested nectar samples were then analysed for ^{13}C content, as described later, to determine whether supplying C4 sucrose caused an increase in nectar sugar ^{13}C content (a less negative $\delta^{13}C$) compared to flowers not supplied with sucrose.

To test the effect of light on excised flower nectar production, three levels of irradiance were provided (no light, 27 μmol m^{-2} s^{-1}, and 88 μmol m^{-2} s^{-1}) to flowers incubated in 30 g l^{-1} sucrose solution. Nectar was collected after 24 h of incubation, with three samples per irradiance level and five flowers per sample. A separate factorial experiment examined the combined effects of light (88 μmol m^{-2} s^{-1}) and external sucrose supply on nectar production by excised flowers, with four treatment combinations (light or darkness, combined with water or sucrose, 30 g l^{-1}) and nine flowers per treatment, with nectar harvested and analysed individually from each flower after 24 h. A second factorial experiment with the same design tested the effect of light and DCMU (light or darkness, combined with water or 100 μM DCMU, without sucrose). The effect of pyridoxal 5′-phosphate (PLP), an inhibitor of the chloroplast envelope triose phosphate translocator (Boschetti & Schmid, 1998; Flugge, 1999), was tested by incubating nine flowers per treatment in 0, 1.5, 10 or 50 mM solutions of PLP, with light (88 μmol m^{-2} s^{-1}). Whilst PLP is likely to have been degraded gradually in the light (Ang, 1979), it is assumed that a proportion was available for uptake via the cut receptacle during the 24 h incubation period.

To test whether CO_2 assimilated within the flower is incorporated into nectar sugars, flowers were incubated in the light as described earlier, and supplied with $^{13}CO_2$ as a gas in the sealed incubation chamber, and simultaneously as 100 mM $H^{13}CO_3^-$ (98% enriched; Sigma-Aldrich, Sydney, NSW, Australia) added to the incubation solution. Both liquid and gaseous routes of supply were used because the gas exchange measurements indicated net outward diffusion of CO_2, even when flowers were exposed to light. The gas was supplied by including a separate dish of saturated citric acid solution within the sealed incubation chamber, then injecting 10 mg of $H^{13}CO_3^-$, dissolved in 250 μl of water, into the dish through a hole in the chamber lid that was sealed immediately afterward. The controls were flowers incubated with no added CO_2 or HCO_3^-, or with $^{12}CO_2$ (non-enriched CO_2 and HCO_3^-). Twelve flowers were incubated per treatment, nectar collected individually from each flower after 24 h, then bulked into three samples (nectar from four flowers per sample) and frozen for later analysis by gas chromatography-mass spectrometry (GC-MS).

Nectar analysis

Nectar was analysed using high-performance liquid chromatography (HPLC) for sugar concentrations (fructose, glucose, sucrose, and DHA). The HPLC system, eluted with ultrapure Barnstead E-Pure water, consisted of: Alltech Elite Degassing system, Waters 515 HPLC pump, Shodex KS guard, KS-801 and KS-802 columns in series, and a Waters 410 refractive index detector. The relationship between HPLC peak area and concentration was linear with $R^2 > 0.98$ for all standard curves. Total sugar (Tsugar, in milligrams per flower) was calculated as the sum of fructose, glucose, and sucrose. Nectar sugar ratios for DHA, fructose (F), glucose (G), and sucrose (S) were estimated as mg mg^{-1}.

Approximate nectar volume (NV) in microlitres per flower was calculated by assuming an average 82.5% recovery of distilled water during rinsing. This recovery was estimated by pipetting and retrieving water from dry flowers without any nectar. Any further volume above this amount was assumed to be nectar. In reality, the efficiency of nectar sampling varies with nectar volume. For simplicity, nectar sugar yields were estimated without attempting to correct for rinsing losses.

The ^{13}C abundance of dried nectar sugars collected from flowers incubated with and without C4 sucrose was measured using a EuropaScientific 20/20 isotope analyser (Waikato Stable Isotope Unit, Hamilton, New Zealand) with samples combusted, separated by GC, and analysed by continuous-flow MS. Samples were referenced to pre-calibrated C4 sucrose that had been cross referenced to the Pee Dee belemnite, and the results expressed as $\delta^{13}C$.

Gas chromatography-mass spectrometry analysis of nectar components

To test whether incubation of flowers in the presence of $^{13}CO_2$ and $H^{13}CO_3^-$ led to enrichment of nectar components with the heavier isotope, nectar sugars and DHA were derivatized after the method of Williams *et al.* (2014); briefly, the sample was divided into two parts, one of which was derivatized with *O*-(2,3,4,5,6-pentafluorobenzyl)hydroxylamine hydrochloride (PFBHA) (derivatization grade, Fluka Analytical, Buchs, Germany) and then per-*O*-trimethylsilylated using 1-(trimethylsilyl)imidazole (TMSI, Thermo Scientific, Scoresby, Australia) for analysis of the DHA and the other part was simply per-*O*-trimethylsilylated for analysis of the sugars in their reducing form. The derivatized samples were analysed using a Hewlett Packard HP 6890 Series gas chromatograph fitted with a Phenomonex Zebron capillary column ZB-5 (30 m × 0.320 mm × 0.25 µm, crosslinked, 5% phenyl polysiloxane and 95% dimethyl polysiloxane) and interfaced to a Hewlett Packard 5973 mass selective detector (1 amu resolution). The carrier gas was helium. The following derivatized ions were selected for investigation for DHA *m/z* 414 $[M - CH_3]^+$, 339 $[M - TMSOH]^+$ and 218 $[M - C_6F_5CH_2ON]^+$ and finally *m/z* 103 $[CH_2OTMS]^+$. For sugars, ions were chosen based upon the fragmentation pathways developed by Kochetkov & Chizhov (1967) for the methyl ether derivatives of reducing sugars, *m/z* 361, 204 and 191 for glucose and for fructose *m/z* 204 and *m/z* 437, the latter is considered to be diagnostic for a two-linked per-*O*-trimethylsilylated ketohexose (Karady & Pines, 1970). The presence of all the ions chosen was confirmed in spectra of derivatized standards. Fragmentation pathways and structures for the heaviest derivatized ion for each of DHA, glucose and fructose are provided in Supporting Information Fig. S1.

Data analysis

All statistical analyses were completed using R (R Core Team, 2020). One-way ANOVA was used to test for differences between nectar sampling frequencies for the flower age experiment, and light levels and PLP concentration in excised flower experiments. For the intact flower shading experiment a randomized complete block ANOVA design was used to test for differences between treatments with plant as the blocking variable. Two-way factorial ANOVA were used for the light × sucrose and light × DCMU excised flower experiments. For the temperature effect experiment, multiple regression was used. Tukey's HSD (honestly significant difference) test was used for all *post hoc* pairwise comparisons, with pairwise comparisons presented when main effects or their interactions were significant ($P < 0.05$). Results from the GC-MS analysis of nectar components were examined using generalized linear models with Poisson errors, and Pearson's chi square to test for significant interactions between treatment (water, $^{12}CO_2$ or $^{13}CO_2$) and mass on the abundances of isotopologues of each of the chosen ions.

Results

Effects of flower age and frequency of nectar sampling

Flower lifespan was approximately 16 d from opening until cessation of nectar production, with petal abscission beginning at 14 d after opening. No nectar was visible immediately after opening, but normally appeared within a day of opening. Nectar flow increased and then decreased during the life of the flower, with a maximum in Tsugar, DHA : Tsugar and nectar volume at 6 d after anthesis (Fig. 2a–c). DHA also reached a maximum at 6 d after anthesis, but the peak in DHA production was narrower than for Tsugar, resulting in a pronounced rise and fall in DHA : Tsugar (Fig. 2a,b,d). The maximum in Tsugar was reflected in the levels of fructose and glucose (making up most of Tsugar) at 6 d after anthesis (Fig. 2a). In contrast to the hexoses and DHA, sucrose levels were maximal at 4 d after anthesis (Fig. 2d). The fructose to glucose ratio (F : G) was also maximal at 4 d after anthesis before steadily decreasing until 16 d (Fig. 2e). The sucrose to Tsugar ratio (S : Tsugar) also decreased steadily from 2 to 14 d (Fig. 2f). The variability of a number of the nectar variables increased later in flower life as nectar volumes declined.

Nectar sampling frequency had no effect on cumulative Tsugar ($P = 0.39$) or nectar volume ($P = 0.11$) over the entire flower lifetime (Table 1). Sampling at 6-d intervals resulted in small but significant increases in DHA : Tsugar, S : Tsugar, S : F, and S : G, compared to either 2-d and 4-d sampling (Table 1). Across all nectar samples collected in this experiment, Tsugar and nectar volume were well correlated ($R^2 = 0.86$).

Temperature effect on nectar flow

In the temperature experiment, flower age (days after anthesis) was a better predictor of all nectar variables than temperature (Fig. 3a; Supporting Information Table S1). Mean temperature from 8 a.m. to 5 p.m. on the day of nectar collection was significantly correlated with some nectar variables (Tsugar, $R^2 = 0.40$, $P = 0.03$; F, $R^2 = 0.40$, $P = 0.03$; G, $R^2 = 0.38$, $P = 0.03$; F : G, $R^2 = 0.37$, $P = 0.03$). Nectar variables were not significantly

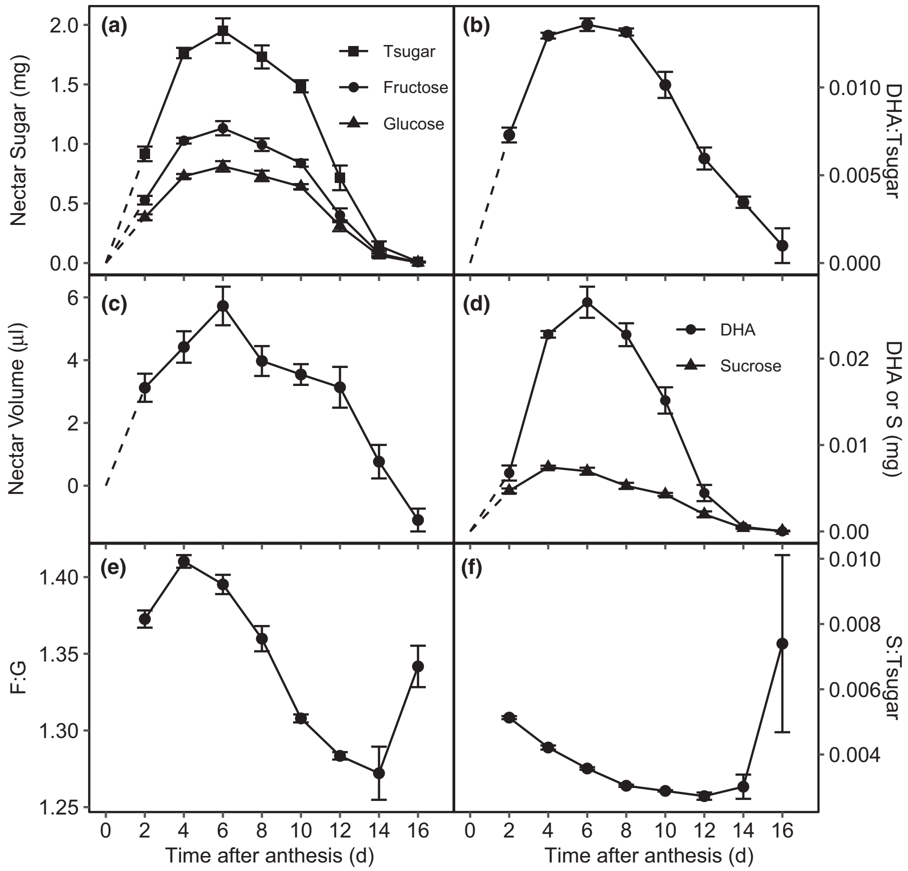

Fig. 2 Flower age effects on nectar traits of intact mānuka (*Leptospermum scoparium*) flowers. (a) Total sugar (Tsugar), fructose, and glucose per flower. (b) Dihydroxyacetone (DHA) to Tsugar ratio (DHA : Tsugar). (c) Nectar volume per flower. (d) DHA and sucrose (S) per flower. (e) Fructose to glucose ratio (F : G). (f) Sucrose to Tsugar ratio (S : Tsugar). Nectar was collected from the same flowers every 2 d for up to 16 d after anthesis (opening). Dashed lines indicate extrapolation from zero nectar present at anthesis. The negative estimated nectar volume and more variable sugar ratios on day 16 are the consequence of low nectar flows. Values are the mean ± 1 SE; $n = 4$ (four nectar samples from 8 to 12 flowers per sample).

Table 1 Effects of nectar sampling frequency on nectar production by mānuka (*Leptospermum scoparium*) flowers while intact on the plant.

	2 d sampling		4 d sampling		6 d sampling		
Tsugar (mg)	8.72 ± 0.10	A	8.55 ± 0.12	A	8.50 ± 0.09	A	ns
DHA (mg)	0.0990 ± 0.0017	AB	0.0970 ± 0.0016	A	0.106 ± 0.002	B	**
DHA : Tsugar	0.0114 ± 0.0001	A	0.0114 ± 0.0001	A	0.0125 ± 0.0002	B	***
F (mg)	5.01 ± 0.06	A	4.90 ± 0.06	A	4.87 ± 0.05	A	ns
G (mg)	3.68 ± 0.04	A	3.62 ± 0.06	A	3.60 ± 0.04	A	ns
F : G	1.360 ± 0.002	A	1.350 ± 0.004	A	1.360 ± 0.003	A	ns
S (mg)	0.0311 ± 0.0005	A	0.0314 ± 0.0005	A	0.0326 ± 0.0003	A	ns
S : Tsugar	0.00357 ± 0.00002	A	0.00368 ± 0.00004	A	0.00383 ± 0.00002	B	**
NV (µl)	23.6 ± 1.1	A	22.2 ± 0.9	A	20.9 ± 0.4	A	ns

Nectar was collected from the same flowers every 2, 4, or 6 d. Values are the mean final total amounts or the ratios of final total amounts per flower produced over the entire flower lifetime.
Tsugar, total sugar; DHA, dihydroxyacetone; DHA : Tsugar, the ratio of DHA to Tsugar; F, fructose; G, glucose; F : G, the ratio of fructose to glucose; S, sucrose; S : Tsugar, the ratio of sucrose to Tsugar; NV, nectar volume; Values are mean ± 1 SE; $n = 4$–6 samples per treatment, 10–12 flowers per sample.
***, $P < 0.001$; **, $P < 0.01$; *, $P < 0.05$; ns, not significant. Letters (A or B) indicate significant pairwise differences between treatments ($P < 0.05$).

correlated with temperature when average temperature for the entire 24-h period, the morning, or the night time hours were used. Multiple regression with days after anthesis and temperature from 8 a.m. to 5 p.m. as predictors resulted in a slightly better model for Tsugar, F, G, F : G, and S, compared to using simple regression (Table S1). Normalizing Tsugar by flower age (using data from Fig. 2a) resulted in a stronger correlation with temperature (Fig. 3b).

Light effect on nectar flow of attached flowers

Shading of individual flowers resulted in significant changes in all nectar variables compared to unshaded treatments (Table 2). Shaded flowers produced less sugar and DHA, but the reduction in DHA was proportionally larger, resulting in a decreased DHA : Tsugar in nectar of shaded flowers (Table 2). Reducing evaporation with plastic film almost doubled nectar volume, but

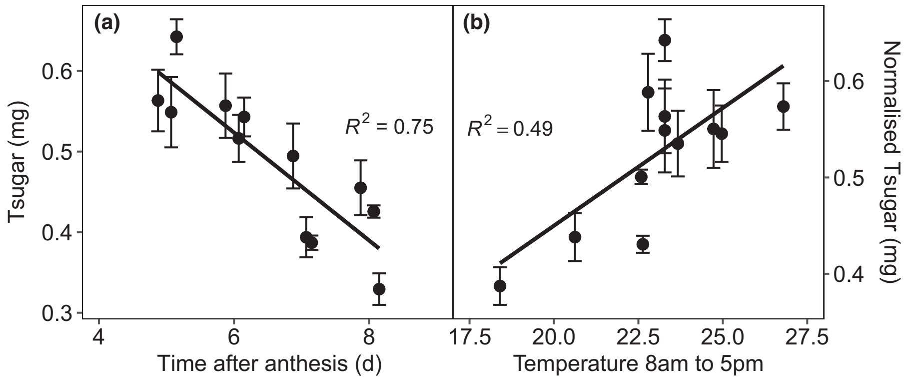

Fig. 3 The effect of flower age and temperature on nectar production by intact mānuka (*Leptospermum scoparium*) flowers on plants subjected to short-term (24 h) differences in temperature. (a) Total nectar sugar (Tsugar) as a function of flower age, regardless of temperature. Flower age was the best predictor of Tsugar and all other nectar traits. (b) Tsugar normalized for flower age as a function of temperature from 8 a.m. to 5 p.m. Values are the mean ± 1 SE; $n = 4$ or 5 (four or five nectar samples from 10 flowers per sample).

Table 2 Nectar production by mānuka (*Leptospermum scoparium*) flowers while intact on the plant and left either uncovered, covered in transparent film (reduced evaporation but did not exclude light), or covered with opaque aluminium foil (reduced evaporation and exclusion of light).

	Uncovered		Clear plastic film		Opaque foil		
Tsugar (mg)	4.18 ± 0.42	A	4.38 ± 0.29	A	1.31 ± 0.33	B	***
DHA (mg)	0.0551 ± 0.0049	A	0.0672 ± 0.0026	A	0.0116 ± 0.0024	B	**
DHA : Tsugar	0.0132 ± 0.0002	A	0.0154 ± 0.0010	B	0.00904 ± 0.00055	C	**
F (mg)	2.44 ± 0.22	A	2.57 ± 0.15	A	0.793 ± 0.190	B	***
G (mg)	1.73 ± 0.20	A	1.79 ± 0.14	A	0.516 ± 0.147	B	**
F : G	1.42 ± 0.04	A	1.44 ± 0.03	A	1.57 ± 0.07	B	*
S (mg)	0.0147 ± 0.0033	A	0.0153 ± 0.0028	A	0.00358 ± 0.00149	B	**
S : Tsugar	0.00345 ± 0.00056	A	0.00343 ± 0.00042	A	0.00253 ± 0.00039	B	**
NV (μl)	9.73 ± 0.65	A	17.3 ± 0.8	B	4.23 ± 0.8	C	***

Coverings were applied only to individual flowers, and not to the leaves. Values are the mean total amounts or ratios of total amounts of nectar components per flower, produced over an average of 7 d from flower opening.
Tsugar, total sugar; DHA, dihydroxyacetone; DHA : Tsugar, the ratio of DHA to Tsugar; F, fructose; G, glucose; F : G, the ratio of fructose to glucose; S, sucrose; S : Tsugar, the ratio of sucrose to Tsugar; NV, nectar volume; Values are mean ± 1 SE; $n = 3$ samples per treatment, 6–7 flowers per sample.
***, $P < 0.001$; **, $P < 0.01$; *, $P < 0.05$. Letters (A, B or C) indicate significant pairwise differences between treatments ($P < 0.05$).

had little effect on the total amounts or relative contributions of the individual nectar sugars. Excluding light had an independent effect on nectar production compared to reducing evaporation alone, because nectar volume halved rather than increased, and only shading affected all other nectar composition variables. The nectary surface of shaded flowers were light green in colour at the time of nectar collection (similar in appearance to a newly opened flower), whilst in unshaded flowers it had become dark red.

Photosynthesis occurs in mānuka nectaries

Net assimilation of CO_2 by excised flowers exhibited a typical saturating photosynthetic response to light, except that assimilation remained negative even at the highest levels of PPFD (Fig. 4a). Removing a proportion of the nongreen tissues (sepals, petals and stamens) made this curve less negative, but did not alter the response to light (Fig. 4a). Assimilation by excised flowers was relatively insensitive to ambient CO_2 concentration (c_a), increasing from −2 to −1 μmol CO_2 m^{-2} s^{-1} as c_a was increased from 50 to 1200 μmol mol^{-1} (data not shown). Electron transport rate, estimated from chlorophyll fluorescence measurements, also exhibited a normal photosynthetic response to light in both leaves and flowers, with the two organs reaching similar potential rates of electron transport per unit area at saturation (Fig. 4b). When chlorophyll fluorescence was compared between flowers with green (younger or more shaded) and red (older or more sun exposed) nectaries, there was no difference in the response of electron transport to light (not shown). Incubation of excised flowers with their cut peduncle in water containing 100 μM DCMU caused a collapse in the effective quantum yield of photosystem II measured at the nectary surface within 1 h of the start of incubation (Fig. 4c). In contrast, the quantum yield of flowers incubated in water remained unchanged after 24 h.

Nectar composition responds to light and supplied sucrose in excised flowers

Nectar production by excised flowers was similar, but not identical, to attached flowers. Across all experiments, attached flower nectar sugar composition was fructose (58–65%), glucose (37–44%), DHA (0.2–1.6%), and sucrose (0.1–0.6%). Excised flower

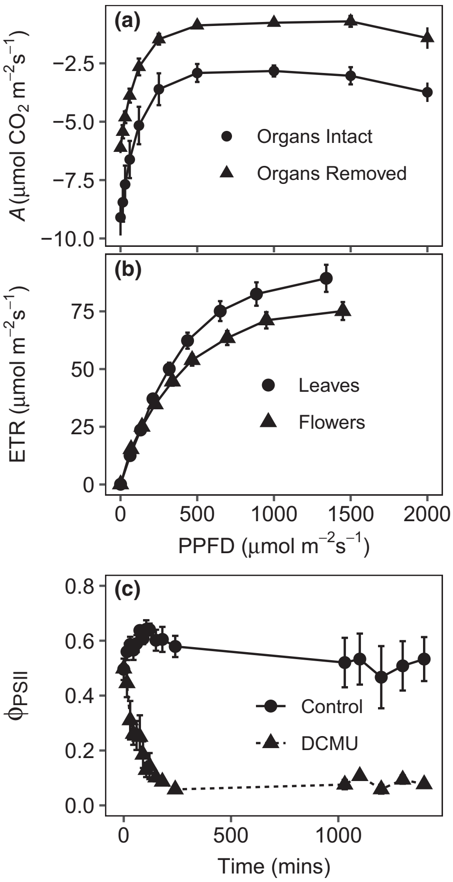

Fig. 4 The photosynthetic properties of mānuka (*Leptospermum scoparium*) flowers. (a) The response of net CO_2 assimilation (A) to photosynthetic photon flux density (PPFD) by intact flowers, or flowers with organs (sepals, petals and stamens) removed. Data were combined for flowers with green (younger) and (older) red hypanthiums, with no difference in photosynthetic response detected between the two forms ($n = 7$ response curves for intact flowers, three for organs removed). (b) The response of electron transport rate (ETR) to PPFD by intact flowers (red hypanthiums) and leaves ($n = 10$ response curves). (c) The effective quantum yield of photosystem II (Φ_{PSII}) as a function of time for excised flowers incubated in water (control) or 100 µM 3-(3,4-dichlorophenyl)-1,1-dimethylurea (DCMU). Values are the mean ± 1 SE.

nectar composition was fructose (51–63%), glucose (35–44%), DHA (1.0–3.5%) and sucrose (0.4–3.1%).

Excised flowers continued to produce nectar for at least 24 h after excision. Tsugar, DHA, DHA : Tsugar, and nectar volume all increased significantly with increasing PPFD during incubation (Fig. 5a–d), whereas F : G and S : Tsugar were unaffected (Fig. 5e,f). In a separate factorial experiment testing the effects of light and supplied sucrose (30 g l^{-1}) on nectar production by excised flowers, light increased Tsugar and DHA ($P < 0.05$ for both variables) but not DHA : Tsugar ($P = 0.28$) (Fig. 6a–c). Supplying sucrose increased Tsugar and decreased DHA : Tsugar ($P < 0.05$ and $P < 0.005$, respectively), but did not affect DHA ($P = 0.16$) (Fig. 6a–c). There was no significant interaction between light and sucrose for any nectar variable ($P > 0.05$). The $\delta^{13}C$ signature of nectar solids collected from excised flowers (−21.45 ± 0.46‰) supplied with C4 sucrose (−11.97‰) was less negative (*t*-test, $P < 0.01$, $n = 3$) than the signature of nectar from intact flowers (−25.01 ± 0.23‰), indicating that a proportion of the supplied sucrose was being incorporated into the nectar produced by the excised flowers.

Inhibiting nectary photosynthesis affects nectar composition

A factorial experiment testing the effects of light and 100 µM DCMU on excised flower nectar production found a significant interaction for Tsugar ($P < 0.001$) and DHA ($P < 0.001$), and a near-significant interaction for DHA : Tsugar ($P = 0.06$). Light increased Tsugar ($P < 0.001$) and DHA ($P < 0.001$) both in the presence and absence of DCMU, but did not affect DHA : Tsugar ($P = 0.37$). DCMU in the light decreased Tsugar ($P < 0.05$), DHA ($P < 0.01$), and DHA : Tsugar ($P < 0.05$), but had no effect in the dark (Fig. 6d–f). PLP supplied in the incubation solution in the light had no effect on Tsugar (Fig. 6g) at any of the tested concentrations, but decreased DHA and hence DHA : Tsugar at concentrations of 10 and 50 mM (Fig. 6h,i).

Carbon dioxide supplied to flowers is incorporated into nectar sugars and DHA

Excised flowers incubated with $^{13}CO_2$ and $H^{13}CO_3^-$ produced nectar DHA, fructose and glucose with clear increases in the proportions of heavier isotopologues in their mass spectra (Fig. 7). Significant interactions ($P < 0.001$) were detected between the effects of treatment (with or without added $^{13}CO_2$ and $H^{13}CO_3^-$) and mass on isotopologue abundance for all of the ions chosen as characteristic for the compounds of interest. This result indicates strong mass shifts from natural ^{13}C abundance towards heavier isotopologues, caused by increased levels of substitution by the heavier ^{13}C isotope, including substitution of up to at least four of the carbons of glucose and fructose, and all three of the carbons of DHA (Fig. 7). For the purposes of this experiment, increases in the proportions of the positively displaced isotopologue signals relative to the unenriched chosen ion signal demonstrates incorporation of the inorganic label into nectar DHA and sugars by photosynthesis within the excised flower.

Discussion

Nectary photosynthesis contributes to nectar sugars

Our results provide strong evidence for a significant contribution by nectary chloroplasts to floral nectar production by mānuka. The best supported models of nectar biosynthesis emphasize phloem-supplied carbohydrates stored as starch in nectary parenchyma, that is then hydrolysed to form the precursors of nectar sugar immediately prior to anthesis (Roy *et al*., 2017). However, many flower parts are photosynthetic (Bazzaz *et al*., 1979), and more species than not may have green nectaries that are capable of contributing carbohydrates directly to nectar production (Pacini *et al*., 2003; Lüttge, 2013). In the present study, the clear effects of light and inhibitors of photosynthesis on nectar flow, and the rapid incorporation into nectar sugars of $^{13}CO_2$

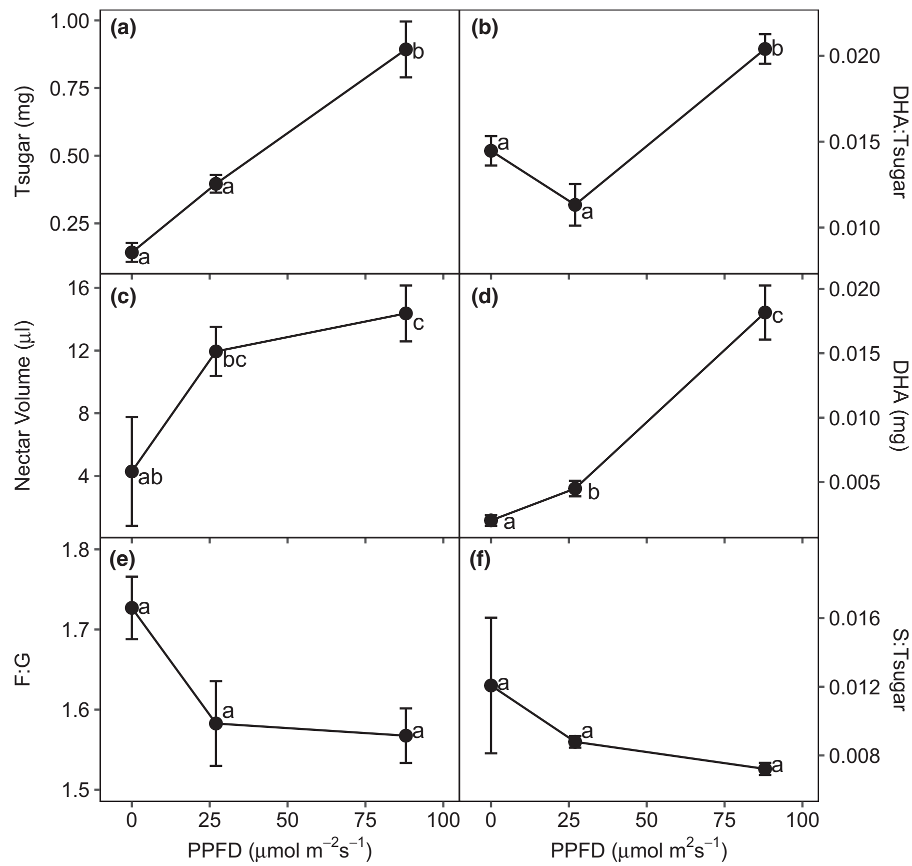

Fig. 5 The effect of photosynthetic photon flux density (PPFD) on nectar production by excised mānuka (*Leptospermum scoparium*) flowers incubated under controlled conditions. (a) Total nectar sugar (Tsugar). (b) Dihydroxyacetone to Tsugar ratio (DHA : Tsugar). (c) Nectar volume. (d) Dihydroxyacetone (DHA. (e) Fructose to glucose ratio (F : G). (f) Sucrose to total sugar ratio (S : Tsugar). Values are the mean ± 1 SE, $n = 3$ (three nectar samples from four or five flowers). Values with different lowercase letters indicate significant differences between light levels (Tukey's HSD, $P < 0.05$).

supplied to the flower, provide direct evidence that nectary photosynthesis contributes a measurable proportion of the nectar sugars produced by mānuka. A role for nectary chloroplasts in nectar production may explain many aspects of variation in nectar composition within and between species that have green nectaries. For mānuka, this includes an explanation for the origin of nectar DHA: as a derivative of triose-phosphate produced by chloroplasts in green nectary cells.

What is the role of nectary chloroplasts, and how much carbon could their photosynthesis contribute to nectar production? Lüttge (2013) used chlorophyll fluorescence measurements to demonstrate that the electron transport capacity of green nectaries was similar to that of leaves for the same species. The potential electron transport rates for mānuka leaves and floral nectaries were also similar to each other, but net CO_2 assimilation by mānuka flowers was negative because the majority of tissues within the gas exchange cuvette (including the gynoecium and developing ovules) were nongreen. The reduction in respiration with irradiance indicated a light saturated assimilation rate for the nectary surface of approximately 5 µmol CO_2 m^{-2} s^{-1}. Scaling to hexose equivalents (Southwick, 1984; Lüttge, 2013), based on a 12 h day and an average nectary surface area of 33 mm^2, yields a maximum sugar production of 0.21 mg d^{-1}, or approximately 20% of peak daily nectar production by flowers from the same plants. Whilst significant, this indicates that nectar production relies on a combination of assimilate imported via the phloem and sugars fixed locally in the nectary.

Green nectaries and their chloroplasts are unlikely to be analogous to green leaf tissue in their functioning. The anatomy of green nectaries differs markedly from leaves, with a low proportion of intercellular space (Davis *et al.*, 1986; Vesprini *et al.*, 1999; Vezza *et al.*, 2006; Nocentini *et al.*, 2012) and poorly developed grana thylakoids compared to leaf chloroplasts (Nepi, 2007; Lüttge, 2013). The insensitivity of nectary photosynthesis to ambient CO_2 concentration (the present study) suggests that nectary chloroplasts, unlike those of leaves, rely primarily on re-fixation of respired CO_2. In addition to supplying assimilate for nectar, another suggested role for nectary chloroplasts is the production of reducing equivalents and adenosine triphosphate (ATP) for the nectar redox cycle and other respiratory demands (Lüttge, 2013). We also propose that nectary photosynthesis could be involved in regulation of sucrose biosynthesis from phloem-derived assimilate in response to light (see later), even if the direct contribution to nectar from assimilation within the nectary itself is not large. This mechanism would contribute to coordination between nectar biosynthesis and the foraging activity of diurnal pollinators. Finally, nectary chloroplasts may also supply reductant and carbon skeletons for the biosynthesis of other nectar components, including the DHA present in mānuka nectar.

A model of nectar production by green nectaries

We propose a modified model of nectar production for long-lived, green nectaries with nectary stomata that lack starch

New Phytologist

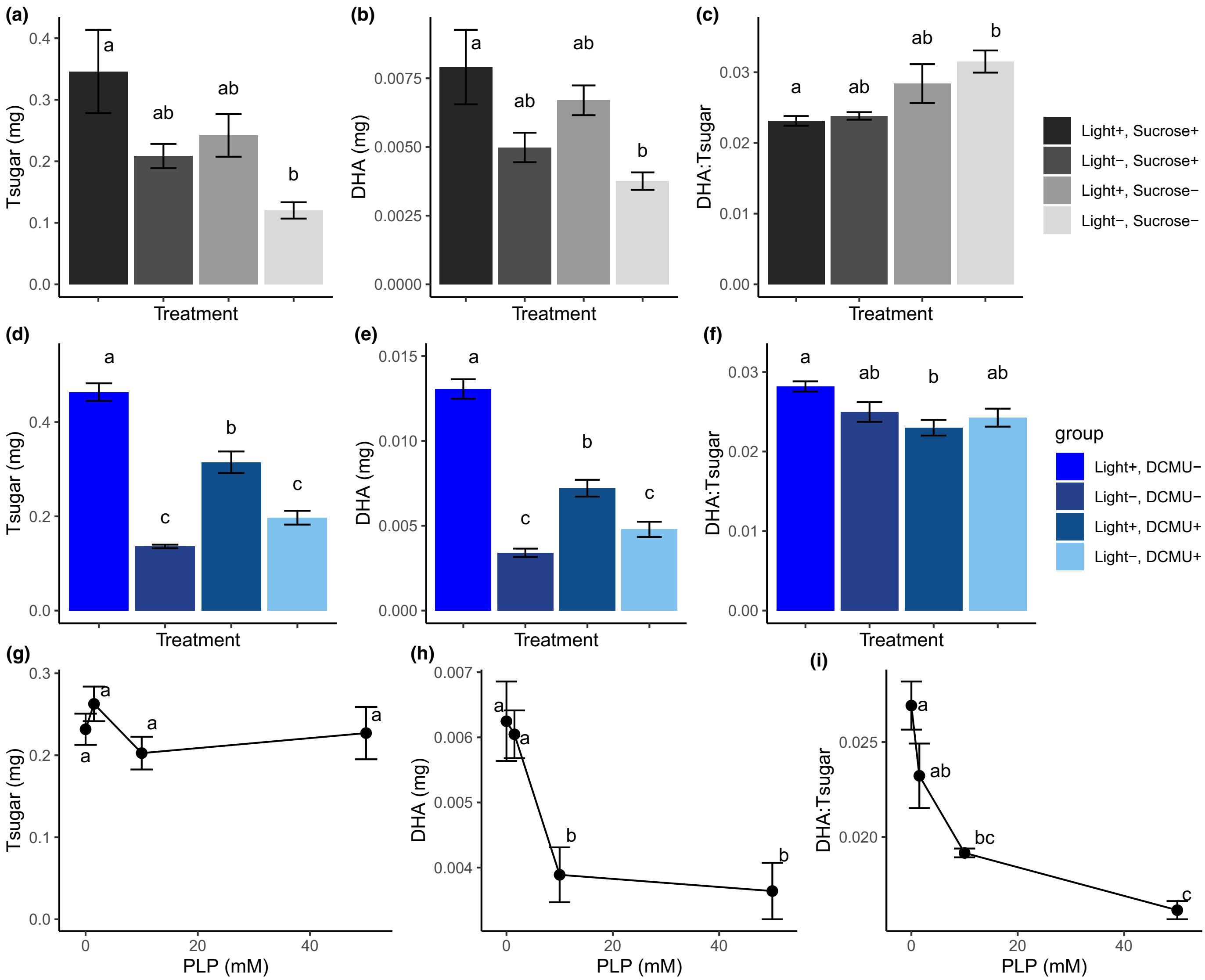

Fig. 6 Nectar total sugar (Tsugar), dihydroxyacetone (DHA), and DHA to total sugar ratio (DHA : Tsugar) for excised mānuka (*Leptospermum scoparium*) flowers in three experiments. (a–c) Factorial test of the effects of light and sucrose (30 g l^{-1}) supplied in the incubation solution. (d–f) Factorial test of the effects of light and 100 μM 3-(3,4-dichlorophenyl)-1,1-dimethylurea (DCMU) supplied in the incubation solution. (g–i) The effects of pyridoxal 5′-phosphate (PLP) supplied at a range of concentrations in the incubation solution. In all experiments, light+ indicates incubation with light at 88 μmol m^{-2} s^{-1} photosynthetic photon flux density (PPFD), and light− indicates incubation with no light. Values are the mean ± 1 SE, $n = 9$ flowers. Values with different lowercase letters indicate significant differences between treatments or concentrations (Tukey's HSD, $P < 0.05$).

accumulation (Fig. 8), by incorporating a role for nectary photosynthesis into existing models of nectary carbohydrate metabolism (Lin *et al.*, 2014; Roy *et al.*, 2017). Strong evidence has been presented that the final stages of eccrine floral nectar secretion usually involves sucrose synthesis by sucrose phosphate synthase (SPS), efflux of sucrose via the sucrose transporter SWEET9, and extracellular cleavage of sucrose to hexoses by cell wall invertase (CWIN4) in the case of hexose-rich nectars (Roy *et al.*, 2017), like that produced by mānuka. In our modified model (Fig. 8), carbohydrates for nectar sugars are supplied from nectary photosynthesis and from phloem-imported sugars, without intervening storage as starch. As occurs in leaf mesophyll cells during the day, dihydroxyacetone phosphate (DHAP) produced by the Calvin cycle and exported from chloroplasts by the triose phosphate transporter can enter glycolysis, or contribute to sucrose synthesis via gluconeogenesis and the hexose phosphate pool (Buchanan, 2015). Increasing cytosolic triose phosphate and decreasing inorganic phosphate (Pi) concentrations caused by illumination are known regulatory signals in leaves that promote upregulation of the gluconeogenic pathway and an enhanced flux of locally-fixed carbon towards the hexose phosphate pool (MacRae & Lunn, 2006). Elevated hexose phosphate and decreased Pi concentrations should promote SPS activity via allosteric and post-translational regulation, and increase the rate of sucrose synthesis (Winter & Huber, 2000). These properties of SPS provide a potential link between illumination, chloroplast photosynthetic activity, and upregulation of nectar production from both phloem and plastid derived sources of sugar.

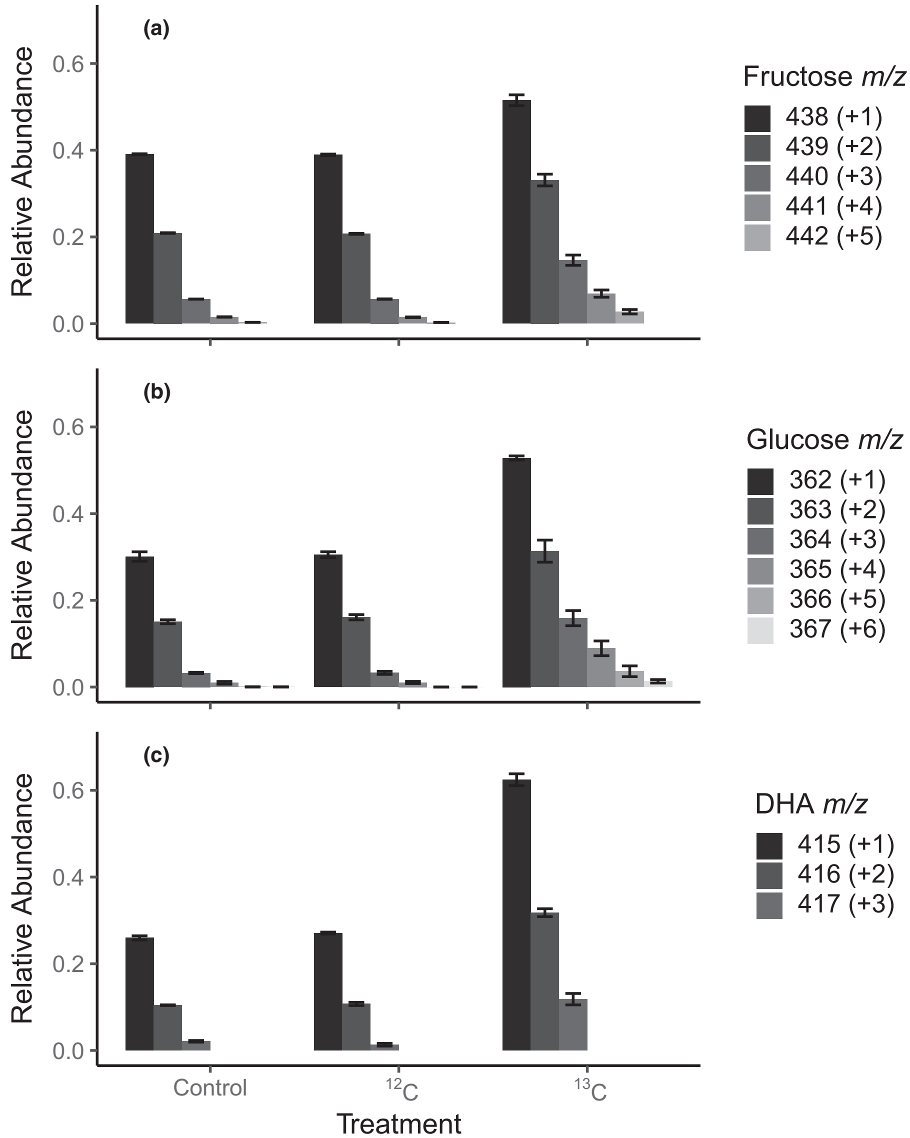

Fig. 7 Mass spectrometer measured abundances of derivative isotopologues with mass shifts between +1 and +6, expressed relative to the abundance of the unenriched chosen ions for fructose, glucose and dihydroxyacetone (DHA), in nectar samples collected from excised mānuka (*Leptospermum scoparium*) flowers incubated with ambient CO_2 (control), added ^{12}C bicarbonate and CO_2, or added ^{13}C bicarbonate and CO_2. For clarity, only the results for the heaviest chosen ion for each compound are provided (see Methods section; fructose *m*/*z* 437, glucose *m*/*z* 361, DHA *m*/*z* 414), and the relative abundances of the unenriched chosen ions (1.0 by definition) are not shown. For all chosen ions there were significant increases in abundance of isotopologues with higher *m*/*z* in response to addition of ^{13}C, indicating enrichment of fructose, glucose and DHA (generalized linear models, $P < 0.001$). Values are the mean ± 1 SE, $n = 3$ nectar samples per treatment, four flowers per sample.

Illumination of nectary chloroplasts could act as an amplifier for nectar production, in addition to driving photosynthetic assimilation of a proportion of nectary sugars. Evidence for the role of light in regulating nectar flow comes from the strong effect of excluding light on total nectar sugars (40% to 80% reductions in nectar sugars; Table 2; Figs 5, 6), and significant effects of light on all measured aspects of nectar composition (Table 2). This effect of light was larger than the estimated potential contribution of nectary photosynthesis to total nectar sugar production, and cannot be attributed to light-independent endogenous circadian rhythms because it was also observed in excised flowers held in continuous light or darkness. It is also relevant to note that previous studies have observed effects of illumination on floral nectar production by a range of species and nectary types, but have manipulated or measured illumination of the entire shoot or plant, including the leaves, and have concluded that light driven alterations in phloem transport to the nectary were responsible for changes in nectar flow (e.g. Kenoyer, 1917; Shuel, 1952; O'Brien *et al.*, 1996).

Origin of dihydroxyacetone in *Leptospermum*

Recognition of the involvement of chloroplasts in nectar production also provides a hypothesis for the potential origin of the DHA present in the nectar of mānuka and other species of *Leptospermum*. Increases in nectar DHA in response to light, and decreases in response to inhibitors of photosystem II and the chloroplast triose phosphate transporter and external sucrose supply (Table 2; Figs 5, 6), suggest a connection between nectar DHA and cytosolic or chloroplastic triose phosphate (DHAP) pools. Light will increase triose phosphate concentrations and the flux through these pools, whilst inhibition of photosynthesis and external sucrose supply should have the opposite effect (MacRae & Lunn, 2006). In this study it is not known whether PLP supplied to excised flowers at high concentrations had a general inibitory effect on cellular metabolism, rather than acting as a specific inhibitor of the chloroplast triose phosphate transporter. While this treatment did cause a decrease in nectar DHA content

New Phytologist

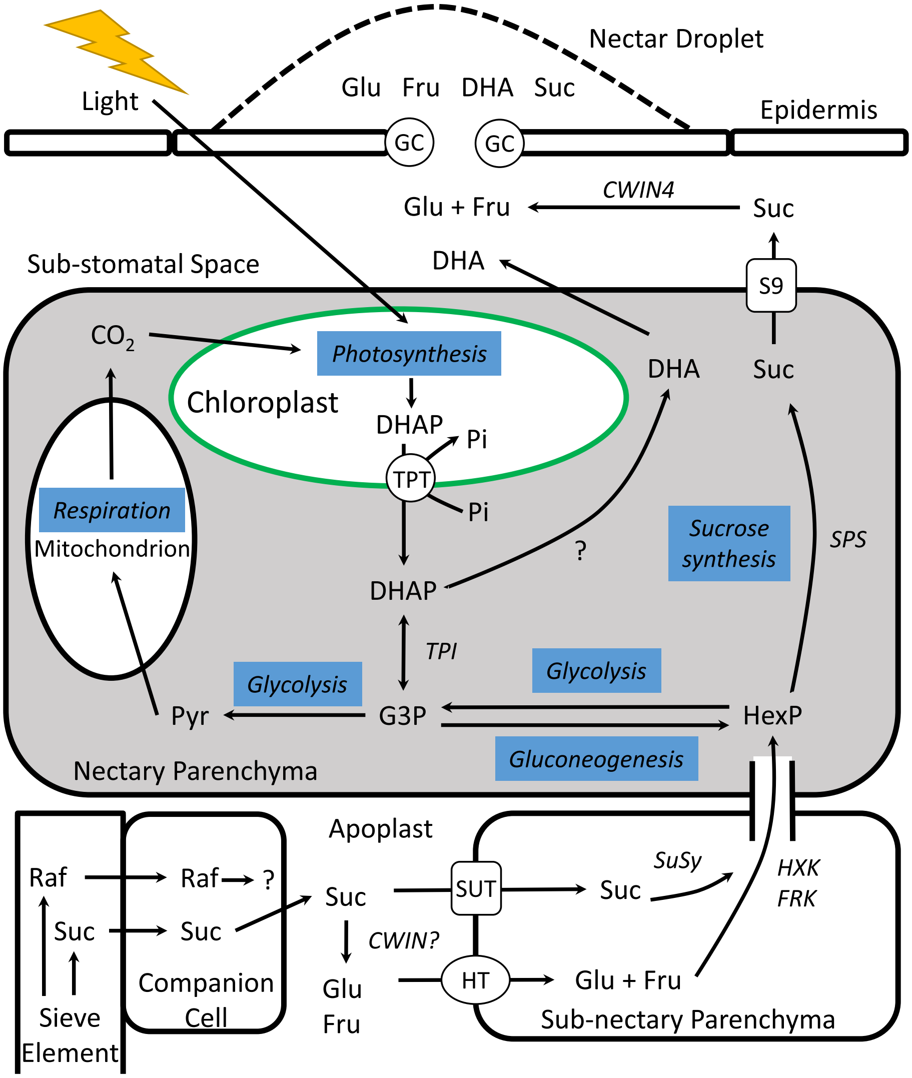

Fig. 8 A proposed model for floral nectar production by mānuka (*Leptospermum scoparium*) and other species with green nectaries, combining elements of established models (Wenzler *et al*., 2008; Lin *et al*., 2014; Roy *et al*., 2017), with results from the present study. In this model, the nectary contains chloroplasts (green) but lacks starch accumulation by amyloplasts prior to anthesis. Sucrose (Suc) and raffinose (Raf) are transported to the nectary via the phloem, and unloaded through an apoplastic pathway to the sub-nectary parenchyma. Sucrose uptake may involve sucrose uptake transporters (SUTs), or cleavage by cell wall invertase (CWIN) to glucose and fructose, followed by uptake by hexose transporters (HTs). The fate of raffinose (present in the phloem of mānuka and other Myrtaceae) is unknown, but likely involves cleavage to other sugars (e.g. Suc and galactose), before exiting the phloem (Ma *et al*., 2019). Unloaded sugars then enter the hexose phosphate (HexP) pool and primary metabolic pathways (blue) in nectary parenchyma via sucrose synthase (SuSy), hexokinase (HXK) or fructokinase (FRK). Photosynthesis by nectary chloroplasts also contributes to the cytoplasmic HexP pool through export of dihydroxyacetone phosphate (DHAP) via the chloroplast-envelope triose phosphate transporter (TPT). DHAP is isomerized to glyceraldehyde-3-phosphate by triose phosphate isomerase (TPI), and further converted to HexP by gluconeogenesis, or to pyruvate (Pyr) by glycolysis. Abundant mitochondria and elevated respiratory activity within the nectary and other floral tissues create a CO_2 rich environment for photosynthesis. In mānuka and other species of *Leptospermum*, a fraction of the DHAP pool is dephosphorylated by an unknown enzyme (?) and diffuses in trace amounts into the apoplast and nectar. Sucrose for nectar secretion is produced from HexP by the sucrose synthesis pathway, with sucrose phosphate synthase (SPS) catalysing the key regulatory step. Sucrose is secreted to the nectary sub-stomatal space by the sucrose efflux transporter SWEET9 (S9), and cleaved to nectar hexoses by cell wall invertase (CWIN4). Osmotic gradients result in the accumulation of water (not shown) and exudation of nectar via nectary stomata and their guard cells (GCs). The primary difference between this and earlier models is the inclusion of photosynthesis by chloroplasts, and their contribution to sucrose biosynthesis by the same pathway that operates in leaf mesophyll cells in the light. As occurs in leaves, SPS activity and sucrose synthesis can be upregulated by the effects of photosynthesis on levels of cytoplasmic phosphate (Pi) and triose phosphate (see text for further explanation).

without affecting total nectar production (Fig. 6), further research on the photosynthetic properties of the nectary is needed to determine how this effect arose. However, transfer of label from $^{13}CO_2$ into all three carbons of nectar DHA by nectary photosynthesis (Fig. 7) provides strong evidence that nectar DHA is derived, either directly or indirectly, from cellular pools of DHAP. This observation does not exclude a microbial origin for nectar DHA in mānuka (Williams *et al.*, 2014), but the microbial explanation is less parsimonious because it requires that a product of nectary photosynthesis be transferred to an endophytic or nectar dwelling microbe, before conversion to DHA. A role for nectary photosynthesis may also explain changes in hexose, sucrose and DHA ratios with flower age as the consequence of developmental changes in nectary photosynthetic activity and the sources of sugars for nectar synthesis (phloem, temporary storage or chloroplasts). The similar but narrower timing of the nectar DHA maximum, compared to the other nectar sugars, suggests a peak in nectary photosynthesis following the opening of the flower and exposure of the nectary to light (Fig. 2). Nectar DHA need not be entirely sourced from nectary photosynthesis, because triose phosphate pools are part of normal cellular metabolism, with or without photosynthesis. Therefore, nectar DHA was not completely eliminated by darkening flowers (Table 2).

Whilst the results presented here provide evidence for a link between nectary photosynthesis and nectar sugars, an origin for nectar DHA from within nectary triose-phosphate pools still requires an explanation for how DHAP is dephosphorylated to form DHA. Furthermore, why is DHA only observed as a measurable component of nectar within a sub-clade of the *Leptospermum* genus (Norton *et al.*, 2015; Williams *et al.*, 2018), rather than all species with green nectaries? Nectary photosynthesis could be a more significant contributor to nectar flow in these species, or it is possible that members of this *Leptospermum* clade share an allele for a phosphatase with higher-than-normal activity towards DHAP (Fig. 8). Sugar phosphatases are ubiquitous (Buchanan, 2015), and lax specificity or variable levels of side activity towards structurally similar substrates are not unusual (Collard *et al.*, 2016; Flügel *et al.*, 2017). Once produced, free DHA is likely to exhibit higher membrane permeability than DHA-P (Naftalin & Smith, 1987), and could enter the apoplast and nectar in trace amounts by facilitated or simple diffusion across the plasma membrane of nectary cells (Pavlovic-Djuranovic *et al.*, 2006; Gomes *et al.*, 2009).

Effects of flower age, temperature and resorption

Flower age, light and temperature are important sources of variation in nectar production by mānuka. The amount and composition of nectar was highly variable in all experiments, as previously observed for mānuka (Clearwater *et al.*, 2018; Smallfield *et al.*, 2018; Noe *et al.*, 2019) and other species (Pacini & Nepi, 2007). Like other species, an important cause of this variation in all nectar variables was flower age, with more than two-fold changes in Tsugar, DHA, and DHA : Tsugar from flower opening to the end of nectar flow (Fig. 2). Increasing temperature had small but positive effects on Tsugar, but was less important than light exposure of the nectary. Nectar sampling frequency had no effect on total sugar, and little effect on other nectar variables over the flower lifetime, suggesting that stimulation of nectar flow by nectar removal, and nectar resorption, were relatively unimportant for the mānuka genotype used in these experiments (Clearwater *et al.*, 2018). A combination of flower age and other environmental variables may therefore explain a significant proportion of the high levels of plant to plant variability in nectar traits observed for wild and cultivated mānuka (Williams *et al.*, 2014; Clearwater *et al.*, 2018; Noe *et al.*, 2019). Future sampling protocols for mānuka nectar, a crucial aspect of plant selection for honey production, should consider flower age as an influential determinant of nectar amount and composition.

In conclusion, we have demonstrated a significant role for photosynthesis by nectary chloroplasts in nectar production in a species with green nectaries. For mānuka, this finding supports the hypothesis that nectar DHA is derived from DHAP produced as an intermediate in the metabolism of photosynthetic nectary parenchyma. An important role for illumination of the nectary, in addition to flower age and temperature, will be no surprise to apiarists who observe that sunshine following rainfall are the best conditions for high nectar flow during peak flowering in mānuka and other species with similar floral nectaries. Future studies of the mechanism of eccrine floral nectar secretion would benefit from the inclusion of a model species with green nectaries to provide understanding of the importance of phloem import vs storage and photosynthesis within the nectary itself for nectar flow and composition. Further investigations of nectar production by mānuka should include a test of the hypothesized origin of nectar DHA from within nectary primary metabolism, including the potential role of a nectary sugar phosphatase in *Leptospermum* species that share the nectar DHA trait.

Acknowledgements

Colin Monk and Lynne Baxter provided support in the laboratory and glasshouses. STN was supported by the University of Waikato, Auckland Botanical Society (Lucy Cranwell Student Grant for Botanical Research), the Māori Education Trust, and Tūhoe Education Contributions. Project support was provided by KiwiNet (PreSeed Accelerator Fund), and the NZ Ministry of Business, Innovation and Employment Endeavour Fund (Programme C09X1608). Three anonymous reviewers and the Associate Editor Teresa Fitzpatrick are thanked for their valuable comments on an earlier version of the manuscript.

Author contributions

MJC, STN, MM-H and SJR planned and designed the research. MJC, STN, G-LT, SG, JM and SAO-D performed the experiments and analysed the data. MJC and STN wrote the manuscript with contributions from the other authors. MJC and STN contributed equally.

ORCID

Michael J. Clearwater https://orcid.org/0000-0002-8563-0671
Merilyn Manley-Harris https://orcid.org/0000-0001-5795-0208
Stevie T. Noe https://orcid.org/0000-0002-5159-7463
Sylvester A. Obeng-Darko https://orcid.org/0000-0002-0769-5939
Sarah J. Richardson https://orcid.org/0000-0002-4097-0381

Data availability

Data available on request due to ethical restrictions.

References

Adams CJ, Boult CH, Deadman BJ, Farr JM, Grainger MNC, Manley-Harris M, Snow MJ. 2008. Isolation by HPLC and characterisation of the bioactive fraction of New Zealand manuka (*Leptospermum scoparium*) honey. *Carbohydrate Research* **343**: 651–659.

Adams CJ, Manley-Harris M, Molan PC. 2009. The origin of methylglyoxal in New Zealand manuka (*Leptospermum scoparium*) honey. *Carbohydrate Research* **344**: 1050–1053.

Ang CY. 1979. Stability of three forms of vitamin B6 to laboratory light conditions. *Journal – Association of Official Analytical Chemists* **62**: 1170–1173.

Bazzaz FA, Carlson RW, Harper JL. 1979. Contribution to reproductive effort by photosynthesis of flowers and fruits. *Nature* **279**: 554.

Bernardello G. 2007. A systematic survey of floral nectaries. In: Nicolson SW, Nepi M, Pacini E, eds. *Nectaries and Nectar*. Dordrecht, the Netherlands: Springer, 19–128.

Boschetti A, Schmid K. 1998. Energy supply for ATP-synthase deficient chloroplasts of *Chlamydomonas reinhardii*. *Plant and Cell Physiology* **39**: 160–168.

Buchanan BB. 2015. *Biochemistry and molecular biology of plants*. Hoboken, NJ, USA: Wiley.

Burge GK, Bicknell RA, Dobson BG. 1996. Postharvest treatments to increase water uptake and the vase life of *Leptospermum scoparium* Forst. *New Zealand Journal of Crop and Horticultural Science* **24**: 371–378.

Chalcoff VR, Aizen MA, Galetto L. 2006. Nectar concentration and composition of 26 species from the temperate forest of South America. *Annals of Botany* **97**: 413–421.

Clearwater MJ, Revell M, Noe S, Manley-Harris M. 2018. Influence of genotype, floral stage, and water stress on floral nectar yield and composition of mānuka (*Leptospermum scoparium*). *Annals of Botany* **121**: 501–512.

Collard F, Baldin F, Gerin I, Bolsée J, Noël G, Graff J, Veiga-da-Cunha M, Stroobant V, Vertommen D, Houddane A *et al.* 2016. A conserved phosphatase destroys toxic glycolytic side products in mammals and yeast. *Nature Chemical Biology* **12**: 601.

Davis AR, Peterson RL, Shuel RW. 1986. Anatomy and vasculature of the floral nectaries of *Brassica napus* (Brassicaceae). *Canadian Journal of Botany* **64**: 2508–2516.

Davis AR, Peterson RL, Shuel RW. 1988. Vasculature and ultrastructure of the floral and stipular nectaries of *Vicia faba* (Leguminosae). *Canadian Journal of Botany* **66**: 1435–1448.

Dawson M. 2010. A History of *Leptospermum scoparium* in cultivation: garden selections. *New Zealand Garden Journal* **13**: 2–9.

Flügel F, Timm S, Arrivault S, Florian A, Stitt M, Fernie AR, Bauwe H. 2017. The photorespiratory metabolite 2-phosphoglycolate regulates photosynthesis and starch accumulation in *Arabidopsis*. *Plant Cell* **29**: 2537.

Flugge UI. 1999. Phosphate translocators in plastids. *Annual Review of Plant Physiology and Plant Molecular Biology* **50**: 27–45.

Gomes D, Agasse A, Thiebaud P, Delrot S, Geros H, Chaumont F. 2009. Aquaporins are multifunctional water and solute transporters highly divergent in living organisms. *Biochimica et Biophysica Acta – Biomembranes* **1788**: 1213–1228.

Heil M. 2011. Nectar: generation, regulation, and ecological functions. *Trends in Plant Science* **16**: 191–200.

Horner HT, Healy RA, Ren G, Fritz D, Klyne A, Seames C, Thornburg RW. 2007. Amyloplast to chromoplast conversion in developing ornamental tobacco floral nectaries provides sugar for nectar and antioxidants for protection. *American Journal of Botany* **94**: 12–24.

Karady S, Pines SH. 1970. Mass spectrometry of the trimethylsilyl ethers of 2-ketohexoses. *Tetrahedron* **26**: 4527–4536.

Kenoyer LA. 1917. Environmental influences on nectar secretion. *Botanical Gazette* **63**: 249–265.

Kochetkov NK, Chizhov OS. 1967. Mass spectrometry of carbohydrate derivatives. In: Wolfrom ML, Tipson RS, eds. *Advances in carbohydrate chemistry, vol. 21*. New York, NY, USA: Academic Press, 39–93.

Kram BW, Carter CJ. 2009. *Arabidopsis thaliana* as a model for functional nectary analysis. *Sexual Plant Reproduction* **22**: 235–246.

Lin IW, Sosso D, Chen L-Q, Gase K, Kim S-G, Kessler D, Klinkenberg PM, Gorder MK, Hou B-H, Qu X-Q *et al.* 2014. Nectar secretion requires sucrose phosphate synthases and the sugar transporter SWEET9. *Nature* **508**: 546–549.

Lüttge U. 2013. Green nectaries: the role of photosynthesis in secretion. *Botanical Journal of the Linnean Society* **173**: 1–11.

Ma S, Li Y, Li X, Sui X, Zhang Z. 2019. Phloem unloading strategies and mechanisms in crop fruits. *Journal of Plant Growth Regulation* **38**: 494–500.

Macauley S, McNeil B, Harvey LM. 2001. The genus *Gluconobacter* and its applications in biotechnology. *Critical Reviews in Biotechnology* **21**: 1–25.

MacRae EA, Lunn J. 2006. Control of sucrose biosynthesis. In: Plaxton W, McManus M eds. *Annual plant reviews Vol. 22 control of primary metabolism in plants*. Oxford, UK: Blackwell Publishing, 234–257.

Mallick SA. 2000. Technique for washing nectar from the flowers of Tasmanian leatherwood (*Eucryphia lucida*) Eucryphiaceae. *Austral Ecology* **25**: 210–212.

Mavric E, Wittmann S, Barth G, Henle T. 2008. Identification and quantification of methylglyoxal as the dominant antibacterial constituent of Manuka (*Leptospermum scoparium*) honeys from New Zealand. *Molecular Nutrition & Food Research* **52**: 483–489.

Naftalin RJ, Smith PM. 1987. A model for accelerated uptake and accumulation of sugars arising from phosphorylation at the inner surface of the cell membrane. *Biochimica et Biophysica Acta – Biomembranes* **897**: 93–111.

Nepi M. 2007. Nectary structure and ultrastructure. In: Nicolson SW, Nepi M, Pacini E, eds. *Nectaries and Nectar*. Dordrecht, the Netherlands: Springer, 129–166.

Nepi M. 2017. New perspectives in nectar evolution and ecology: simple alimentary reward or a complex multiorganism interaction? *Acta Agrobotanica* **70**: 12.

Nicolson SW, Thornburg RW. 2007. Nectar chemistry. In: Nicolson SW, Nepi M, Pacini E, eds. *Nectaries and Nectar*. Dordrecht, the Netherlands: Springer, 215–263.

Nocentini D, Pacini E, Guarnieri M, Nepi M. 2012. Flower morphology, nectar traits and pollinators of *Cerinthe major* (Boraginaceae-Lithospermeae). *Flora* **207**: 186–196.

Noe S, Manley-Harris M, Clearwater MJ. 2019. Floral nectar of wild mānuka (*Leptospermum scoparium*) varies more among plants than among sites. *New Zealand Journal of Crop and Horticultural Science* **47**: 282–296.

Norton AM, McKenzie LN, Brooks PR, Pappalardo LJ. 2015. Quantitation of dihydroxyacetone in Australian *Leptospermum* nectar via high-performance liquid chromatography. *Journal of Agricultural and Food Chemistry* **63**: 6513–6517.

Obeng-Darko SA. 2018. *Anatomical and molecular basis of floral nectar secretion by mānuka (Leptospermum scoparium)*. MSc Thesis. University of Waikato, Hamilton, New Zealand.

O'Brien SP, Loveys BR, Grant WJR. 1996. Ultrastructure and function of floral nectaries of *Chamelaucium uncinatum* (Myrtaceae). *Annals of Botany* **78**: 189–196.

Pacini E, Nepi M, Vesprini JL. 2003. Nectar biodiversity: a short review. *Plant Systematics and Evolution* **238**: 7–21.

Pacini E, Nepi M. 2007. Nectar production and presentation. In: Nicolson SW, Nepi M, Pacini E, eds. *Nectaries and Nectar*. Dordrecht, the Netherlands: Springer, 167–214.

Pacini E, Nicolson SW. 2007. Introduction. In: Nicolson SW, Nepi M, Pacini E, eds. *Nectaries and nectar*. Dordrecht, the Netherlands: Springer, 1–18.

Parachnowitsch AL, Manson JS, Sletvold N. 2019. Evolutionary ecology of nectar. *Annals of Botany* **123**: 247–261.

Pavlovic-Djuranovic S, Kun JFJ, Schultz JE, Beitz E. 2006. Dihydroxyacetone and methylglyoxal as permeants of the *Plasmodium* aquaglyceroporin inhibit parasite proliferation. *Biochimica et Biophysica Acta – Biomembranes* **1758**: 1012–1017.

Percival MS. 1961. Types of nectar in angiosperms. *New Phytologist* **60**: 235–281.

R Core Team. 2020. *R: a language and environment for statistical computing*. Vienna, Austria: R Foundation for Statistical Computing, v.4.0.2 [WWW document] URL https://www.R-project.org/ [accessed 8 April 2020].

Ren G, Healy RA, Klyne AM, Horner HT, James MG, Thornburg RW. 2007. Transient starch metabolism in ornamental tobacco floral nectaries regulates nectar composition and release. *Plant Science* **173**: 277–290.

Roy R, Schmitt AJ, Thomas JB, Carter CJ. 2017. Nectar biology: from molecules to ecosystems. *Plant Science* **262**: 148–164.

Rußmayer H, Buchetics M, Gruber C, Valli M, Grillitsch K, Modarres G, Guerrasio R, Klavins K, Neubauer S, Drexler H *et al.* 2015. Systems-level organization of yeast methylotrophic lifestyle. *BMC Biology* **13**: 25.

Shuel RW. 1952. Some factors affecting nectar secretion in red clover. *Plant Physiology* **27**: 95–110.

Smallfield BM, Joyce NI, van Klink JW. 2018. Developmental and compositional changes in *Leptospermum scoparium* nectar and their relevance to manuka honey bioactives and markers. *New Zealand Journal of Botany* **56**: 183–197.

Solhaug EM, Johnson E, Carter CJ. 2019. Carbohydrate metabolism and signaling in squash nectaries and nectar throughout floral maturation. *Plant Physiology* **180**: 1930–1946.

Southwick EE. 1984. Photosynthate allocation to floral nectar: a neglected energy investment. *Ecology* **65**: 1775–1779.

Thornburg RW. 2007. Molecular biology of the *Nicotiana* floral nectary. In: Nicolson SW, Nepi M, Pacini E, eds. *Nectaries and nectar*. Dordrecht, the Netherlands: Springer, 265–288.

Thrimawithana AH, Jones D, Hilario E, Grierson E, Ngo HM, Liachko I, Sullivan S, Bilton TP, Jacobs JME, Bicknell R *et al.* 2019. A whole genome assembly of *Leptospermum scoparium* (Myrtaceae) for manuka research. *New Zealand Journal of Crop and Horticultural Science* **47**: 233–260.

Vesprini JL, Nepi M, Pacini E. 1999. Nectary structure, nectar secretion patterns and nectar composition in two *Helleborus* species. *Plant Biology* **1**: 560–568.

Vezza M, Nepi M, Guarnieri M, Artese D, Rascio N, Pacini E. 2006. Ivy (*Hedera helix* L.) flower nectar and nectary ecophysiology. *International Journal of Plant Sciences* **167**: 519–527.

Wenzler M, Hölscher D, Oerther T, Schneider B. 2008. Nectar formation and floral nectary anatomy of *Anigozanthos flavidus*: a combined magnetic resonance imaging and spectroscopy study. *Journal of Experimental Botany* **59**: 3425–3434.

Wicaksono WA, Jones EE, Monk J, Ridgway HJ. 2016. The bacterial signature of *Leptospermum scoparium* (mānuka) reveals core and accessory communities with bioactive properties. *PLoS ONE* **11**: e0163717.

Wicaksono WA, Jones EE, Sansom CE, Perry NB, Monk J, Black A, Ridgway HJ. 2017. Indigenous bacteria enhance growth and modify essential oil content in *Leptospermum scoparium* (mānuka). *New Zealand Journal of Botany* **55**: 306–317.

Williams SD, King J, Revell M, Manley-Harris M, Balks M, Janusch F, Kiefer M, Clearwater M, Brooks P, Dawson M. 2014. Regional, annual, and individual variations in the dihydroxyacetone content of the nectar of manuka (*Leptospermum scoparium*) in New Zealand. *Journal of Agricultural and Food Chemistry* **62**: 10332–10340.

Williams SD, Pappalardo L, Bishop J, Brooks PR. 2018. Dihydroxyacetone production in the nectar of Australian *Leptospermum* is species dependent. *Journal of Agricultural and Food Chemistry* **66**: 11133–11140.

Winter H, Huber SC. 2000. Regulation of sucrose metabolism in higher plants: localization and regulation of activity of key enzymes. *Critical Reviews in Plant Sciences* **19**: 31–67.

Witt T, Jürgens A, Gottsberger G. 2013. Nectar sugar composition of European Caryophylloideae (Caryophyllaceae) in relation to flower length, pollination biology and phylogeny. *Journal of Evolutionary Biology* **26**: 2244–2259.

Wolff D. 2006. Nectar sugar composition and volumes of 47 species of Gentianales from a southern Ecuadorian montane forest. *Annals of Botany* **97**: 767–777.

Supporting Information

Additional Supporting Information may be found online in the Supporting Information section at the end of the article.

Fig. S1 Fragmentation pathways and structures for derivatized ions chosen for observation of mass shifts, for each of DHA, glucose and fructose.

Table S1 Simple and multiple regression results with flower age and day-time temperature as predictors of nectar composition.

Please note: Wiley Blackwell are not responsible for the content or functionality of any Supporting Information supplied by the authors. Any queries (other than missing material) should be directed to the *New Phytologist* Central Office.